

From the Insoluble Dye Indirubin towards Highly Active, Soluble CDK2-Inhibitors

Rolf Jautelat,^{*[a]} Thomas Brumby,^[a] Martina Schäfer,^[b]
Hans Briem,^[c] Gerhard Eisenbrand,^[d]
Stefan Schwahn,^[d] Martin Krüger,^[a] Ulrich Lücking,^[a]
Olaf Prien,^[a] and Gerhard Siemeister^[e]

Dedicated to Prof. Helmut Vorbrüggen on the occasion of his 75th birthday

The natural product indirubin (**1**) is part of the class of indigo dyes, employed by mankind since the Bronze Age for textile coloring.^[1] These indigo dyes were traditionally obtained by processing of precursor compounds occurring in a number of plants and marine animals and consisted mainly of indigo (**5**; blue) with a small percentage of indirubin (**1**; purple). In the course of an intensive effort to prepare synthetic indigo as a further program for the rapidly expanding dye industries, the first total synthesis of indirubin (**1**) was achieved in 1870 by Adolf von Bayer.^[2] Shortly thereafter, the total synthesis of indigo was achieved, and synthetic indigo became a major product of the dye industries. Eventually, this dye chemistry laid the foundation for the first synthetic drugs including ar-sphenamine, acetaminophen, and acetyl salicylic acid.

More than 100 years later in 1979, indirubin was reported in a seminal publication to be the active constituent of a traditional Chinese antileukemia remedy.^[3]

This finding prompted further investigations into the pharmacological properties of the indirubins^[4,5,6] and resulted in a 1999 report by Eisenbrand, Johnson, Meijer, and co-workers, who showed that indirubin and close analogues are ATP-competitive inhibitors of the enzyme CDK2 (**1**: IC₅₀ = 2 μM; see Table 1), a key target in the ongoing search for novel antitumor therapies.^[7,8] This discovery places indirubin in the larger class of ATP-competitive CDK inhibitors of the oxindole family, such as **2**, **3**, and **4** (Scheme 1).^[8,9] In this publication, the X-ray structure of the related indirubin-5-sulfonic acid (**20**; IC₅₀ =

[a] Dr. R. Jautelat, Dr. T. Brumby, Dr. M. Krüger, Dr. U. Lücking, Dr. O. Prien
Medicinal Chemistry, Research Center Europe
Schering AG, 13342 Berlin (Germany)
Fax: (+49) 304-681-8170
E-mail: rolf.jautelat@schering.de

[b] Dr. M. Schäfer
ET/Structural Biology, Research Center Europe
Schering AG, 13342 Berlin (Germany)

[c] Dr. H. Briem
CDCC/Computational Chemistry, Research Center Europe
Schering AG, 13342 Berlin (Germany)

[d] Prof. Dr. G. Eisenbrand, Dr. S. Schwahn
Department of Chemistry
Division of Food Chemistry and Environmental Toxicology
University of Kaiserslautern
Erwin-Schrödinger-Straße 52, 67663 Kaiserslautern (Germany)

[e] Dr. G. Siemeister
Corporate Research, Experimental Oncology
Schering AG, 13342 Berlin (Germany)

Table 1. Physicochemical and pharmacological characterization of indirubin derivatives; see Experimental Section for details on the employed methods.

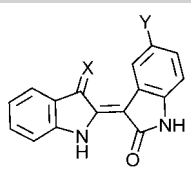
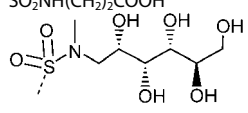
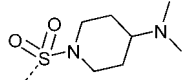
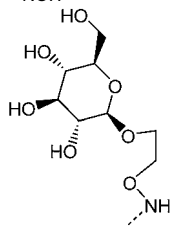
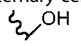
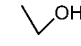
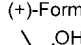
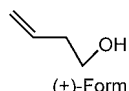
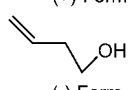
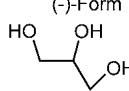
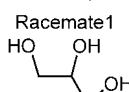
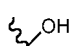
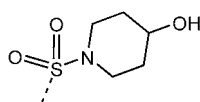
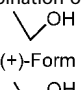
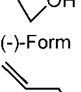
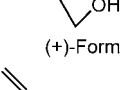
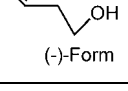
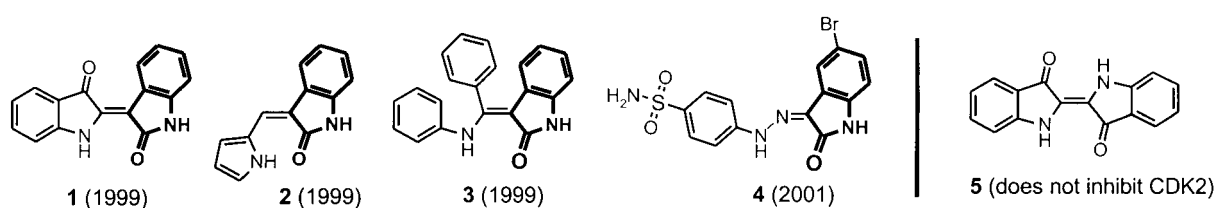
Cpd.	X desired profile	Y	clogD -1 to +5	CDK2 [μM] < 0.1	S_w [mg L^{-1}] > 40	MCF7 [μM] < 1
						
Series A: First exploration of indirubin scaffold						
1	=O	H	2.5	2	< 1	> 10
14	=O	Br	3.7	1	< 1	8
20	=O	SO ₂ OH	-2.1	0.5	n.d.	> 10
8	=O	SO ₂ NMe ₂	2.3	0.04	< 1	> 10
32	=NOH	SO ₂ NMe ₂	2.0	0.04	< 1	0.4
Series B: Polar substituents on 5-sulfonamides						
33	=O	SO ₂ NH(CH ₂) ₂ OH	1.3	0.08	< 1	> 10
34	=O	SO ₂ NH(CH ₂) ₂ COOH	-1.4	1.5	> 40	n.d.
35	=O		-0.3	0.45	34	n.d.
36	=O		1.4	0.02	6	0.5
22	=O	SO ₂ NMe(CH ₂) ₂ N(Me) ₂	1.5	0.01	12	< 0.1
23	=NOH	SO ₂ NMe(CH ₂) ₂ N(Me) ₂	1.2	0.04	18	< 0.1
25		SO ₂ NMe(CH ₂) ₂ N(Me) ₂	-1.1	0.9	n.d.	n.d.
36	as in comp. 25	SO ₂ NMe ₂	-0.2	0.08	5	> 10
Series C: Quaternary center on 3'-position						
26		Br	3.3	3	9	0.9
27a		SO ₂ NMe ₂	1.9	0.07	> 40	0.7
27b	(+)-Form 	SO ₂ NMe ₂	1.9	0.6	16	2.2
29a	(+)-Form 	SO ₂ NMe ₂	2.4	0.09	31	0.2
29b	(-)-Form 	SO ₂ NMe ₂	2.4	4	34	n.d.
31a	Racemate 1 	SO ₂ NMe ₂	0.3	3	n.d.	n.d.
31b	Racemate 2 	SO ₂ NMe ₂	0.3	> 10	n.d.	n.d.
37			1.6	1.6	n.d.	n.d.

Table 1. (Continued)

Cpd.	X desired profile	Y	clogD -1 to +5	CDK2 [μM] < 0.1	S_w [mg L^{-1}] > 40	MCF7 [μM] < 1
Series D: Combination of 3'-quaternary center and polar 5-sulfonamides						
28a	 (+)-Form	$\text{SO}_2\text{NMe}(\text{CH}_2)_2\text{N}(\text{Me})_2$	1.0	0.07	> 40 (710) ^[a]	< 0.1
28b	 (-)-Form	$\text{SO}_2\text{NMe}(\text{CH}_2)_2\text{N}(\text{Me})_2$	1.0	0.4	> 40 (655) ^[a]	n.d.
30a	 (+)-Form	$\text{SO}_2\text{NMe}(\text{CH}_2)_2\text{N}(\text{Me})_2$	1.5	0.04	> 40 (418) ^[a]	< 0.1
30b	 (-)-Form	$\text{SO}_2\text{NMe}(\text{CH}_2)_2\text{N}(\text{Me})_2$	1.5	0.6	> 40 (438) ^[a]	n.d.

[a] Additional solubility values were determined by the flask method (thermodynamic solubility; $S_w(t)$).



Scheme 1. Known ATP-competitive CDK2 inhibitors incorporating the oxindole motive—and indigo; the year that CDK2 activity was first reported for these types of compounds is given in brackets.

0.5 μM ; see Table 1) bound to CDK2 gave the first insight into the binding mode of these novel inhibitor structures incorporating the oxindole motif.^[7]

Taken together, the indirubins were discovered to be a new lead series in the search for therapeutically relevant CDK2 inhibitors. The drawbacks of these early indirubins were those already known: very low aqueous solubility, causing poor absorption and low cellular activity (see Table 1).^[5,7]

Thus, a group from Schering AG, Berlin and the Eisenbrand group set out in a joint effort to prepare indirubin derivatives that could overcome these issues and deliver novel compounds with high CDK2 potency ($\text{IC}_{50} < 0.1 \mu\text{M}$), good water solubility ($S_w > 40 \text{ mg L}^{-1}$), and high activity in suppressing the *in vitro* growth of the MCF7 cancer cell line ($\text{MCF7} < 1 \mu\text{M}$; the desired profile is listed in Table 1) as the prerequisite for further *in vivo* evaluation. In addition, a colorless compound was preferred. This communication highlights the findings of our recent work toward indirubin derivatives with the desired properties.

Only a small number of indirubins are commercially available. Our first entry into this class was thus to follow a well-

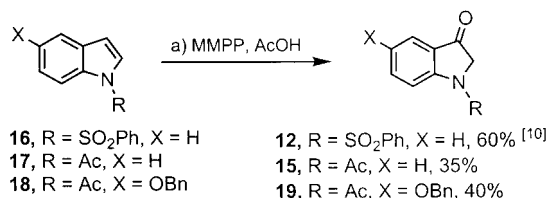
known modular approach towards indirubins by the condensation of an indoxyl equivalent, such as **6**, and an isatin, such as **7** (Table 2). Commonly employed indoxyl derivatives of the indoxyl *O*-acetate (e.g., **6**), indoxyl *N,O*-diacetate (e.g., **9**), and indoxyl *N*-acetate (e.g., **15**) type provided good yields on basic and/or on acidic coupling with different isatins (see Table 2, entries 1, 2, and 5).

To obtain access to more indoxyl derivatives via the large class of commercially available indoles, we first employed a method that allowed for the oxidation of indole *N*-benzenesulfonates (e.g., **16**) into the corresponding indoxyl *N*-benzenesulfonates (e.g., **12**; see Scheme 2).^[10] Attempts to employ these indoxyl *N*-benzenesulfonates in couplings with isatins to yield the corresponding indirubins were successful under basic conditions, but with low yields (Table 2, entry 4). Under acidic conditions such attempts failed (decomposition of the indoxyl species on extended reaction times), since the acidic cleavage of *N*-benzenesulfonates occurs only under harsh conditions and this cleavage is required for the condensation reaction. We therefore modified the protocol and employed a variety of indole *N*-acetates—such as **17** and **18**—as starting materials.

Table 2. Access to indirubins through coupling of indoxyl derivatives with isatins.

No.	Indoxyl	Isatin	Product	Cond. A	Cond. B
				Cond. A: AcOH, HCl conc. (cat.) 80–100°C, 3–4 h	
1	6: R, Y=H, X=OAc	7: A=SO ₂ NMe ₂	8: R=H, A=SO ₂ NMe ₂	98%	93%
2	9: R=H, X, Y=OAc 10: R=Cl, Y=H, X=	7: A=SO ₂ NMe ₂	8: R=H, A=SO ₂ NMe ₂	67%	n.a. ^[a]
3		7: A=SO ₂ NMe ₂	11: R=Cl, A=SO ₂ NMe ₂	86%	n.a. ^[a]
4	12: R=H, X=O, Y=SO ₂ Ph	13: A=Br	14: R=H, A=Br	0%	32%
5	15: R=H, X=O, Y=Ac	13: A=Br	14: R=H, A=Br	70%	59%

[a] n.a.=not applicable.



Scheme 2. Oxidative synthesis of indoxyl *N*-acetates. Reagents and conditions: a) Monoperoxy magnesium phthalate (MMPP; 1 equiv), AcOH, 125°C, 2 h.

This delivered the desired indoxyl *N*-acetates, though in lower yields than the corresponding indoxyl *N*-benzenesulfonates. Not surprisingly, attempts to extend this oxidative method to electron-deficient indole derivatives such as 1-acetyl-5-nitroindole failed.

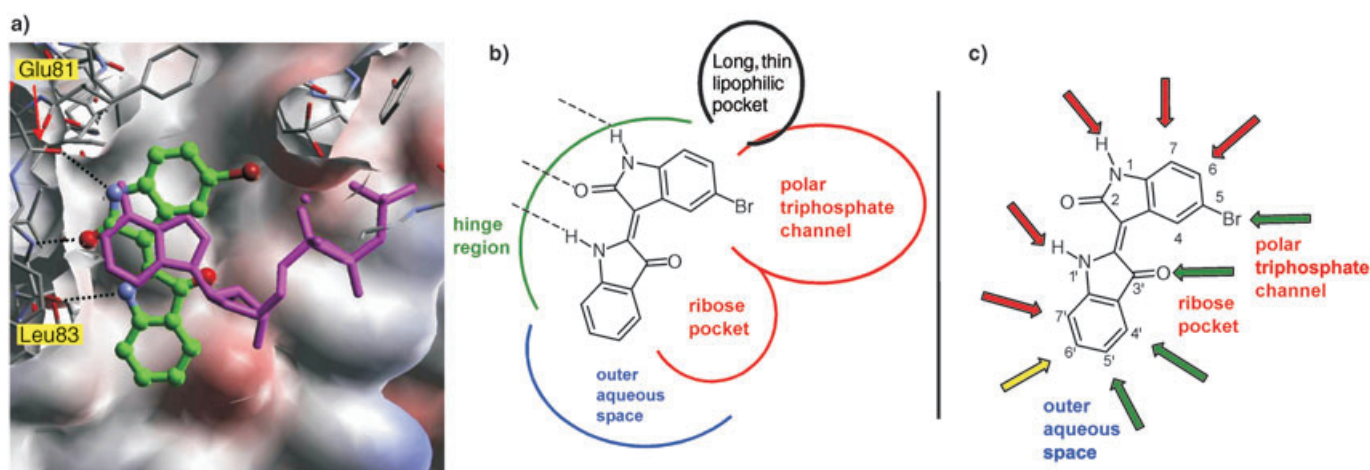


Figure 1. a) Top view of 5-bromoindirubin **14** (color-by-atom) superimposed with ATP (purple) in the ATP binding niche of CDK2. The 5-bromoindirubin binds in the deep, relatively flat pocket of CDK2, and mimics the hydrogen-bond pattern to the hinge region observed in the ATP structure. The position 1 amide donates a hydrogen bond to the backbone carbonyl oxygen of Glu81, whereas the position 2 carbonyl acts as a hydrogen-bond acceptor for the backbone nitrogen of Leu83. The position 1' nitrogen acts as a hydrogen bond donor to the backbone carbonyl oxygen of Leu83. b) Schematic depiction of 5-bromoindirubin in the ATP-binding pocket. c) Display of positions amenable for modifications.

Finally, we were also successful in employing commercially available indoxyl *O*-sugars such as **10** as donor components in the condensation reaction (see Table 2, entry 3).

Series A: First exploration of the indirubin scaffold

With these methods to hand, we prepared a set of explorative indirubin derivatives from the approximately 25 commercially available isatins, the approximately 15 indoxyl derivatives and some custom isatins and indoxyls. The first SARs and SPRs (structure–property relationships) thus generated agreed with the published X-ray data,^[7,11] and with our in-house-

generated X-ray structure of 5-bromoindirubin (**14**) bound to CDK2 (see Figure 1 a).

Only positions 5, 3', 4', and 5' appeared to be readily amenable for substitutions (see Figure 1 c), while substituents in positions 1, 6, 7, 6', and 7' lead to loss of activity (data not shown). The increase in CDK2 potency (by a factor of 25) observed with the dimethylsulfonamide substitution in position 5 of compound **8** lead to a CDK2 IC₅₀ of 0.04 μM (see Table 1). Thus, **8** emerged as a lead structure for further optimization efforts. However, **8**, as well as related close analogues (data not shown), still shared the indirubin “textile-dye property” of aqueous insolubility. This prevented any *in vivo* studies and was also most likely the reason for strong fluctuations of cellular activity in this series (compare **8** and **32**, Table 1), since compounds of very low solubility lead to unpredictable effects

on testing in *in vitro* (and *in vivo*) systems; the compounds precipitate when added to aqueous biological systems, for example, or stick to certain compartments of the cell. To overcome this low solubility, two strategies were examined, based on the empirical Equation (1), that puts the solubility of an organic compound in water ($\log S$) in relation to its affinity to water ($\log D$) and the affinity of the compound to itself (m.p.):^[12]

$$\log S = -\log D - 0.01 \text{ m.p.} \quad (1)$$

Series B: Polar substituents on 5-sulfonamides

The first strategy was to increase the affinity to water (decrease $\log D$) by introducing polar groups—either into the core structure or attached to it. However, this strategy has limitations, as very polar molecules ($\log D < -1$) will no longer passively penetrate physiological lipid bilayers.^[13]

Since lead compound **8** had a $c\log D$ (calculated $\log D$) of 2.3, there was scope left for increasing polarity. In pursuit of this strategy, inspection of the available X-ray data in combination with modeling studies identified the 5-position (pointing towards the polar triphosphate channel), the 3'-position (pointing towards the ribose pocket), and the 5'-position (pointing towards the aqueous surroundings at the end of the pocket) as promising positions to attach polar functionality (see Figure 1b). We expected that these polar side chains would increase not only aqueous solubility but also the affinity to the ATP binding pocket through interaction with the corresponding polar pockets (triphosphate channel, ribose pocket).

First, **1** was converted via the corresponding 5-indirubin-sulfonic acid **20** into the sulfonyl chloride species **21**, which was then treated with large number of nucleophiles, mostly amines, by parallel synthesis techniques (see Scheme 3).

While amino alcohol side chains did not substantially increase the solubilities of these compounds ($S_w < 1 \text{ mg L}^{-1}$ in all cases; example **33** in Table 1), polar amino acid side chains (e.g., **34**) and amino polyols (e.g., **35**) diminished CDK2 potency below our IC_{50} threshold of $0.1 \mu\text{M}$. Finally, utilization of basic diamine side chains gave access to new indirubin derivatives such as **22**, with good CDK2 potency ($0.01 \mu\text{M}$), markedly increased solubility (12 mg L^{-1}), and excellent cellular activity

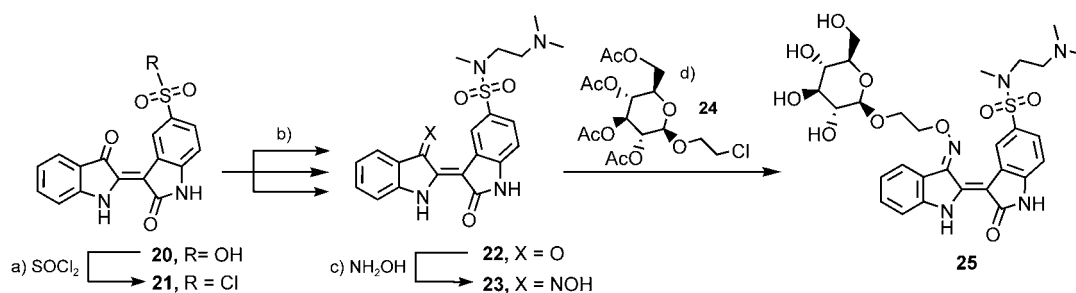
(< $0.1 \mu\text{M}$). The basic sulfonamide **22** was then coupled in the 3'-position with further solubility-increasing elements, namely oxime ethers, firstly by treatment with hydroxylamine to yield **23** and subsequently by treatment under basic conditions with various nucleophiles such as the sugar building block **24**. While the simple oxime derivative **23** displayed a slight increase in solubility (18 mg L^{-1} compared to the 12 mg L^{-1} of the 3'-keto species **22**) and retained its activity, all corresponding oxime ethers (e.g., **25**) displayed unacceptable decreases in CDK2 activity.

All other attempts to substantially increase the solubility of the lead compound **8**, variously through the 3'-position (other oxime ether derivatives) or through the 4'- and 5'-positions, while maintaining CDK potency were unsuccessful (data not shown).

Series C: Deplanarization—quaternary center at the 3'-position

The second strategy was to decrease planarity. Because of the inherent "textile-dye nature" of the indirubins—being completely flat and rigid—these molecules form adhesive crystal packings; this is reflected by the high melting points (> 300°C) of these compounds, which are rather modest in size and polarity.^[14] The probability was therefore high that disturbing the flatness of these molecules should reduce their propensity for tight crystal packing, thus decreasing their melting point and resulting in increased water solubility. Inspection of the X-ray data and corresponding modeling studies revealed the 3'-position as a potential handle through which to "break" the planarity of the indirubins without risking loss of CDK2 potency in the rather flat binding pocket (see Figure 2).

In a first study, a suspension of 5-bromindirubin (**14**) in THF was treated with an excess of methylmagnesium bromide at room temperature (see Scheme 4). Nucleophilic attack took place at the more active 3'-carbonyl group to provide the corresponding tertiary alcohol **26**. Although starting material **14** and product **26** are similar in $c\log D$, they differ strongly in m.p. (> 300°C for **14** but 231°C for **26**) and, nicely following the empirical Equation (1), the "quaternary indirubin" **26** showed—in contrast to **14**—a measurable (!) water solubility of 9 mg L^{-1} (see Table 1).



Scheme 3. Synthesis of basic indirubin sulfonamides. Reagents and conditions: a) SO_2Cl_2 (80 equiv) 80°C , 3 h, 75%; b) $\text{N,N,N'-trimethylethylenediamine}$ (1.8 equiv), DMAP (cat), 60°C , 8 h, 85%; c) NH_2OH (1 equiv), KOH (20 equiv), EtOH, 2 h, reflux, 32%; d) **24** (3.6 equiv), TMG (4 equiv), EtOH, 6 h, reflux, 30% (DMAP = 4-dimethylaminopyridine, TMG = tetramethylguanidine).

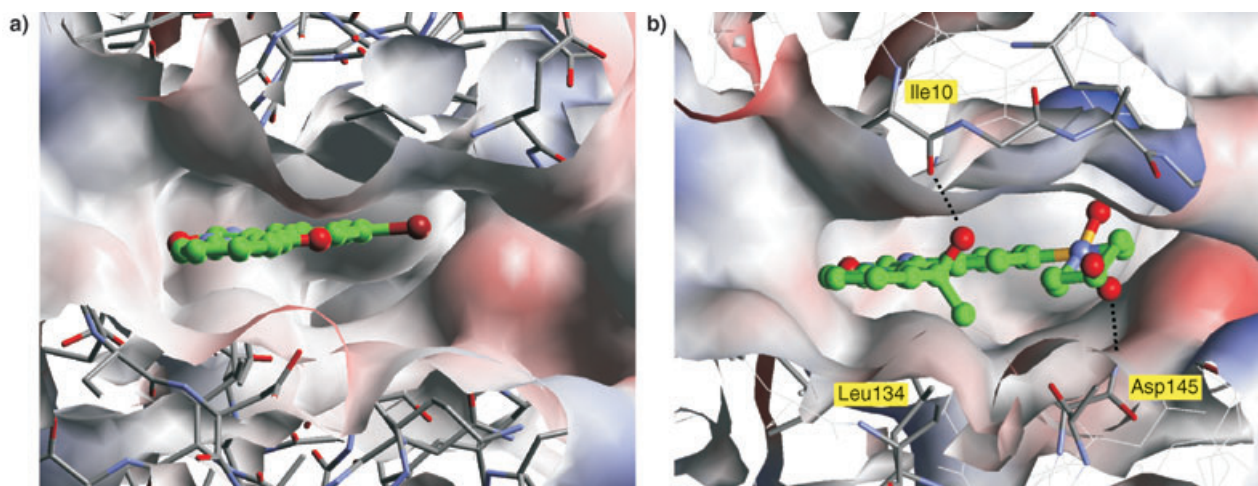
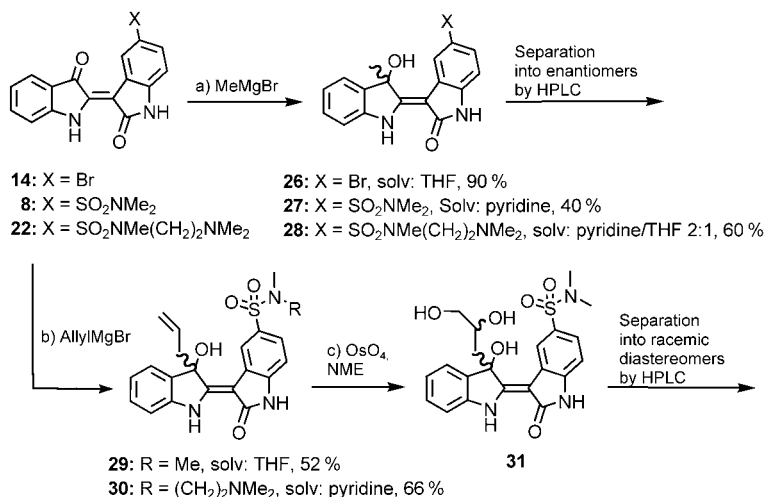


Figure 2. a) Side view of 5-bromoindirubin **14** illustrating the relatively flat cleft of the ATP binding pocket of CDK2. b) The scaffold of the quaternary indirubin **37** is in almost the same position as the 5-bromoindirubin **14** and forms the same hydrogen-bond pattern to the hinge region of CDK2. In addition, the hydroxy oxygen atom in the 3' position forms a weak hydrogen bond to the carbonyl oxygen of Ile10, whereas the methyl group is in the hydrophobic environment of the Leu134 side chain. This interaction pattern suggests that even though the racemate was soaked into the CDK2 crystal, only the *S* form of the quaternary compound has bound. Furthermore, both oxygens of the sulfonamide group are close to the main-chain amide of Asp145 and the side-chain nitrogen of Lys33.



Scheme 4. Generation of quaternary indirubins through Grignard reactions: a) MeMgBr (4–9 equiv; 3 M in ether), 4 → 20 °C, 1 h, solvents and yields specified within the scheme; b) allylmagnesium bromide (6 equiv, 2 M in THF), 10 → 20 °C, 1 h; c) NMO (2.2 equiv), OsO₄, THF/H₂O, RT, 5 h, 62 % (NMO = N-methylmorpholine oxide).

With this result in hand, we set out to prepare numerous “quaternary indirubins”, mainly in combination with 5-sulfonamides (see Scheme 4). Because of the lack of solubility of our starting materials in THF at room temperature, we also employed THF/pyridine mixtures or even pure pyridine as the solvent for the Grignard reactions. The Grignard reaction prevailed in a wide range of yields (see Scheme 4) and transformed the intensely purple starting materials into pale yellow products, as a direct consequence of the disturbance of the extended delocalized π -system through the transformation of the 3'-carbonyl into a tertiary alcohol. The resulting racemic compounds were then separated by chiral HPLC. The CDK2 po-

tencies of these products with 3'-quaternary centers were generally lower than those of the corresponding 3'-keto compounds by factors of 2 to 10, but in many cases still met our threshold of < 0.1 μ M (**27a**: 0.07 μ M, **29a**: 0.09 μ M). In all cases the (+) enantiomer was more active than the (–) enantiomer by a factor of 10 to 50 (vide infra). The solubility was in or above our standard measurement range (**27a** > 40 mg L⁻¹) and the inhibition of tumor cell growth met our criteria (**29a**: 0.7 μ M).

As expected, increased bulk in the near vicinity of the 3'-position lead to decreased binding, since there is only limited space in the binding pocket (data not shown). In an attempt to mimic the ribose pocket of ATP, additional hydroxy groups were introduced into the allyl side chain of **29** under standard dihydroxylation conditions.^[15] However, neither of the racemic diastereomers **31a** and **31b** showed sufficient CDK2 potency (see Table 1).

Our initial assumption regarding the 3'-position, based on the X-ray data and modeling studies, was finally proved correct by obtaining an X-ray of the quaternary indirubin **37** in conjunction with the CDK2 protein. Indirubin **37** was used in a racemic form in the experiment, and the electron density data showed that it was well located in the CDK binding pocket. The newly formed hydrogen bond between the 3'-hydroxy group of **37** and the carbonyl of Ile 10 was readily visible from the X-ray analysis (see Figure 2b). Thus, although one cannot discriminate between the two enantiomers in terms of electron density (a methyl group vs. a hydroxyl group being in the 3'-position) the new hydrogen bond clearly showed that only the 3'*S* form was bound in the ATP pocket of CDK2.

Series D: Combination of 3'-quaternary center and polar 5-sulfonamides

Finally, the combination of increasing polarity in the side chain and decreasing planarity in the core structure propelled the water solubility to values above our standard upper measuring limit of 40 mg L⁻¹; for example, **28a** and **30a** (see Scheme 4 and Table 1). In addition, their water solubilities were determined by a thermodynamic method (flask method), good water solubility being found for both **28a** (710 mg L⁻¹) and **30a** (418 mg L⁻¹)—with the expected trend of a higher solubility for **28a** than for **30a**. These compounds proved to be high in CDK2 potency (**30a**: 0.04 μM) and showed strong antiproliferative activity against the MCF7 cell line (**30a**: <0.1 μM). As observed before, the (+) enantiomers were always of higher activity than their (–) counterparts.

Selectivity of the new indirubin derivatives against other targets

Meijer and co-workers reported a number of indirubins to be low nanomolar inhibitors of glycogen synthase kinase-3β (gsk3).^[16,17] Gsk3 may be involved in a number of diseases, including diabetes, neurodegenerative disorders, inflammation, infectious diseases, and, last but not least, cancer. However, it currently seems that it indeed has multiple roles and thus we were not interested in a gsk3 component of our anticancer CDK2-inhibitors. While the early compounds **14**, **20**, and **32** (see Table 3) show significant to strong gsk3 inhibition—in line

Table 3. Selectivity of the optimized indirubins against several kinases.

Cpd.	CDK2 [μM]	gsk3 [μM]	InsR [μM]	EGFR [μM]	c-kit [μM]	KDR [μM]
Desired profile	<0.1	>10	>10	>10	>10	>10
14	1	0.08	>10	>10	>10	>10
20	0.5	0.3	>10	>10	>10	>10
32	0.04	4	n.d.	n.d.	n.d.	n.d.
28a	0.07	>10	>10	>10	>10	>10
28b	0.4	>10	>10	>10	>10	>10
30a	0.04	>10	>10	>10	>10	>10
30b	0.6	>10	>10	>10	>10	>10

with data on similar compounds already reported—our later compounds **28a/b** and **30a/b** are devoid of this activity (see Table 3). This elimination of gsk3 activity, while maintaining good CDK2 activity, is not compromised by any loss of selectivity against other kinases, such as EGFR, c-kit, InsR, and KDR (see Table 3).

Recently there have been several reports showing that indirubins activate the aryl hydrocarbon receptor (AhR).^[18,19,20,21] AhR, also known as the dioxine receptor, is an orphan nuclear transcription factor, similar to the hormone receptors, that plays an important and long-known role in the regulation of xenobiotic metabolism. AhR activation itself does not lead to toxic or carcinogenic effects, as the known toxins and carcinogens acting via the AhR do so by AhR-induced expression of

specific CYP enzymes, which then “toxify” the initially nontoxic AhR activator, for example, by epoxidation.^[22] In addition, the past decade has brought evidence that the AhR is an active participant in the control of cell homeostasis. In line with these observations, two structure classes acting as AhR agonists have shown potent antitumor activity against breast and mammary tumors in animal studies, while showing low toxicity.^[22,23] For indirubins it has been reported that simple, low-substituted derivatives are potent AhR activators. The cytotoxic effects of indirubins appear to be mediated by CDK2 in an AhR-independent manner. However, several 1-methylindirubins, devoid of any CDK2 (and gsk3) activity, showed strong cytostatic effects.^[21] Thus the AhR-binding properties of indirubins may well contribute to their reported in vivo effects on leukemia. We currently do not possess data on the AhR properties of our advanced indirubin derivatives such as **30a/b**, and further investigations should add valuable pieces to the “AhR puzzle”.

Finally, indirubin (**1**) has been reported to be a nonselective inhibitor of targets other than kinases (β-lactamase, chymotrypsin, malate dehydrogenase) at higher micromolar levels (>20 μM).^[24] This effect is exerted by a nonspecific aggregate formation of indirubin (and also of a number of other nonspecific inhibitors). The mechanism for this aggregate formation is currently unknown, thus we can not exclude the possibility that our advanced indirubin derivatives, such as **30a/b**, may also possess this property and exert it at concentrations well above the 10 μM tested in our assays. However, we can state that the observed low nanomolar CDK2 inhibition of **30a/b** is due to the specific binding at the ATP side, as indicated by the several X-rays of related indirubins in this and other publications, and that the submicromolar concentrations needed for inhibition of cancer cell growth in vitro (<0.1 μM) would make the necessity for a 100-fold higher in vivo concentration unlikely.^[25]

Strongly supported by X-ray data and modeling studies, we have succeeded in deriving from the initial lead compound indirubin (**1**) a number of readily soluble, almost colorless derivatives that potently and selectively inhibit the activity of the CDK2 enzyme and control the growth of MCF7 cancer cells in vitro.^[26] Further results of our investigations into this fascinating class of molecules will be reported in due course.

Experimental Section

Pharmacological characterization of indirubin derivatives CDK2: GST-tagged recombinant human CDK2 kinase (50 ng) complexed with GST-tagged human cyclin E expressed in SF-9 cells (Proqinase, Germany) was incubated for 10 min at 22 °C in the presence of different concentrations of test compounds in a Tris/HCl assay buffer [40 μL, 62.5 mM, pH 8.0, MgCl₂ (10 mM), dithiothreitol (1.0 mM), sodium orthovanadate (0.1 mM), PEG 20000 (0.025% v/v), ATP (0.5 μM), γ-³³P ATP (0.2 μCi per well), calf thymus histone type III S (1 μM, Sigma–Aldrich, Germany), dimethyl sulfoxide (1.25%, v/v), Nonidet P40 (0.05%)]. The reaction was stopped by the addition of a solution of EDTA in water (0.25 M, 10 μL, pH 7.5). A quantity (15 μL) of each reaction mixture was transferred to P30 filter sheets (Wallac, Germany), washed with phosphorous acid (0.5%, 3 × 10 min), and subjected to scintillation counting with MeltiLex A scintillator sheets (Wallac, Germany) and a Micobeta counter

(Wallac, Germany). Half-maximal inhibition (IC_{50}) of CDK2/cyclin E activity was determined as the inhibitor concentration resulting in 50% of substrate phosphorylation between maximal substrate phosphorylation in the presence of solvent and background phosphorylation in the presence of inactivated CDK2.

GSK3 β : Human recombinant gsk3 β (10 mU per well) expressed in SF-9 cells (Upstate Biotech, UK) was incubated for 30 min at 22 °C in the presence of different concentrations of test compounds in a Mops assay buffer [30 μ L, 4 mM, pH 8.0, MgCl₂ (0.5 mM), MnCl₂ (0.5 mM), Mg acetate (2.5 mM), dithiothreitol (1.0 mM), ATP (0.5 μ M), γ -³³P ATP (62.5 nCi per well), biotinylated gsk3 β substrate peptide (4 μ M, Biosynthan, Germany), dimethyl sulfoxide (1.25% v/v), Nonidet P40 (0.002%)]. The reaction was stopped by the addition of Stopp solution [EDTA; 20 μ L, 5 mM, pH 7.5, Triton X100 (0.1%), ATP (50 μ M), streptavidin SPA beads (0.25 mg per well, Amersham, UK)]. The mixture was precipitated by centrifugation at 1500 rpm and subjected to scintillation counting on Topcount equipment. Half-maximal inhibition (IC_{50}) of gsk3 β activity was determined as the inhibitor concentration resulting in 50% of substrate phosphorylation between maximal substrate phosphorylation in the presence of solvent and background phosphorylation in the presence of inactivated gsk3 β .

InsR: GST-tagged recombinant human Ins-R kinase domain (ProQinase, Germany) expressed in SF-9 cells was used as kinase. Biotinylated poly-(Glu,Tyr) (Cis biointernational, France) was used as substrate for the kinase reaction. Ins-R (\approx 15 ng, depending on activity) was incubated for 10 min at 22 °C in the presence of different concentrations of test compounds in a Hepes/NaOH assay buffer [15 μ L, 50 mM, pH 7.5, MgCl₂ (5 mM), MnCl₂ (5 mM), dithiothreitol (1.0 mM), sodium orthovanadate (3 μ M), PEG 20000 (0.025% v/v), ATP (5 μ M), substrate (12 ng), dimethyl sulfoxide (1.5% v/v)]. The reaction was stopped by the addition of a solution of HTRF detection reagents [5 μ L, streptavidine-XL665 (20 ng) and PT66-Eu(K) (5 ng Cis biointernational)] in an aqueous EDTA solution [0.5 M, bovine serum albumin (1% w/v) in HEPES/NaOH, 50 mM, pH 7.0]. The resulting mixture was incubated for a further 2 h at 22 °C to allow the binding of the biotinylated peptide to the streptavidine-XL665, and the amount of phosphorylated product was subsequently evaluated by HTRF measurement in a Rubystar (BMG, Germany).

EGFR: EGFR protein (Sigma, #E2645) affinity purified from human carcinoma A431 cells was used as kinase. Biotinylated poly-(Glu,Ala,Tyr) (Cis biointernational, France) was used as substrate for the kinase reaction. EGFR (0.5 U) was incubated for 20 min at 22 °C in the presence of different concentrations of test compounds in a Hepes/NaOH assay buffer [15 μ L, 50 mM, pH 7.0, MgCl₂ (25 mM), MnCl₂ (5 mM), sodium orthovanadate (0.5 mM), ATP (1 μ M), substrate (34 ng), dimethyl sulfoxide (1.5% v/v)]. The reaction was stopped by the addition of a solution of HTRF detection reagents [streptavidine-XL665 (125 ng) and PT66-Eu(K) (5 ng, 5 μ L; Cis biointernational)] in an aqueous EDTA solution [0.5 M, bovine serum albumin (1% w/v) in HEPES/NaOH, 50 mM, pH 7.0]. The resulting mixture was incubated for a further 2 h at 22 °C to allow the binding of the biotinylated peptide to the streptavidine-XL665 and the amount of phosphorylated product was subsequently evaluated by HTRF measurement in a Rubystar (BMG, Germany).

c-kit: GST-tagged recombinant human c-kit kinase domain expressed in SF-9 cells was used as kinase. Biotinylated poly-(Glu,Tyr) (Cis biointernational, France) was used as substrate for the kinase reaction. c-kit was incubated for 10 min at 22 °C in the presence of different concentrations of test compounds in a Hepes/NaOH assay

buffer [15 μ L, 50 mM, pH 7.0, MgCl₂ (25 mM), MnCl₂ (5 mM), dithiothreitol (1.0 mM), sodium orthovanadate (0.5 mM), ATP (3 μ M), substrate (50 ng), glycerol (10% v/v), dimethyl sulfoxide (1.5% v/v)]. The reaction was stopped by the addition of a solution of HTRF detection reagents [streptavidine-XL665 (100 ng) and PT66-Eu(K) (6 ng, 5 μ L; Cis biointernational) in an aqueous EDTA solution [0.5 M, bovine serum albumin (1% w/v) in HEPES/NaOH, 50 mM, pH 7.0]. The resulting mixture was incubated for a further 2 h at 22 °C to allow the binding of the biotinylated peptide to the streptavidine-XL665, and the amount of phosphorylated product was subsequently evaluated by HTRF measurement in a Rubystar (BMG, Germany).

KDR: GST-tagged recombinant human KDR kinase domain expressed in SF-9 cells was used as kinase. Biotinylated poly-(Glu,Ala,Tyr) (Cis biointernational, France) was used as substrate for the kinase reaction. KDR was incubated for 20 min at 22 °C in the presence of different concentrations of test compounds in a Hepes/NaOH assay buffer [15 μ L, 50 mM, pH 7.0, MgCl₂ (25 mM), MnCl₂ (5 mM), dithiothreitol (1.0 mM), sodium orthovanadate (0.5 mM), ATP (1 μ M), substrate (350 ng), glycerol (10% v/v), dimethyl sulfoxide (1.5% v/v)]. The reaction was stopped by the addition of a solution of HTRF detection reagents [streptavidine-XL665 (175 ng) and PT66-Eu(K) (7.5 ng, 5 μ L; Cis biointernational)] in an aqueous EDTA solution [0.5 M, bovine serum albumin (1% w/v) in HEPES/NaOH (pH 7.0, 50 mM)]. The resulting mixture was incubated for a further 2 h at 22 °C to allow the binding of the biotinylated peptide to the streptavidine-XL665 and the amount of phosphorylated product was subsequently evaluated by HTRF measurement in a Rubystar (BMG, Germany).

MCF7: MCF7 cells (ATCC, USA) were seeded in RPMI 1640 medium (Biochrome, Germany) supplemented with fetal calf serum (10%, PAA, Austria), L-glutamine (2 mM), estradiol (0.1 nM), and insulin (1 U mL⁻¹) at 5000 cells per well in 96-well plates. Cells were allowed to adhere for 24 h, and then fresh growth medium plus compounds were added. The final concentration of the solvent DMSO was 0.5%. After 4 days of continuous incubation, the cells were fixed with glutaraldehyde and stained with crystal violet, and the absorbance was recorded at 595 nm. All measurements were performed in quadruplicate. The values were normalized to the absorbance of solvent-treated cells (= 100%), and the absorbance of a reference plate which was fixed at the time point of compound application (= 0%). Half-maximal growth inhibition (IC_{50}) was determined as compound concentration required to achieve 50% inhibition of cellular growth.

Physicochemical calculations and characterization

clogD: Calculation was performed with the ACD/logD program version 6.0. (Advanced Chemistry Development, Inc, Toronto, Canada)

S_w : This was determined by turbidimetric measurements (kinetic solubility). A solution of the compound in DMSO (10 mM) was added gradually to aqueous buffer. Turbidity was measured by its effect on the transmission of light. The experiment was run at 25 °C in phosphate buffer at pH 7.4. The instrument was a HACH turbidimeter, the software for analysis and evaluation was an in-house program. The system was calibrated with phenanthrene.

$S_w(t)$ (solubility in water determined by the flask method—thermodynamic solubility): A saturated solution of the compound in phosphate buffer at pH 7.4 was stirred at 25 °C for 22 h. The solid was separated by filtration, and the concentration of compound in the solution was determined by quantitative HPLC. HPLC: Waters

2695/PDA. Column: Xterra MSC18 4.6×30 mm. Eluent: A: water/0.025% NH₃, B: CH₃CN/0.025% NH₃. Gradient: 0–3 min 20→80% B, 3–5 min 80% B, 5–6 min 20% B.

Crystallographic data for CDK2 in complexes with compounds 14 and 37: a) CDK2–14 complex: orthorhombic, space group *P*2₁2₁2₁, crystal dimensions 0.1×0.1×0.05 mm³, cell dimensions *a* = 53.685(10), *b* = 71.918(10), *c* = 71.22(10) Å, *V* = 277 684 Å³, *Z* = 4, *T* = 100 K, λ = 0.933 Å (Synchrotron), max. resolution = 1.9 Å, 146 442 reflections collected, of which 20 611 are independent [*R*_{int} = 0.054, Friedel mates are merged], completeness = 97%, *R*₁ = 22.9% for *I* > 2σ(*I*) and *R*_{free} = 29.7%, b) CDK2–37 complex: orthorhombic, space group *P*2₁2₁2₁, crystal dimensions 0.3×0.3×0.2 mm³, cell dimensions *a* = 53.679(2), *b* = 69.526(3), *c* = 71.168(3) Å, *V* = 260 657 Å³, *Z* = 4, *T* = 100 K, λ = 1.54178 Å (Cu-radiation), max. resolution = 2.6 Å, 73 463 reflections collected, of which 8542 are independent [*R*_{int} = 0.091, Friedel mates are merged], *R*₁ = 26.7% for *I* > 2σ(*I*) and *R*_{free} = 32.2%.

Crystals of CDK2 were grown at 20°C by vapor diffusion. CDK2 (1–298) at 5–7 mg mL⁻¹ was mixed and equilibrated against PEG 3350 (10%), ammonium acetate (0.2 M) at pH 7.8 (Hepes). Compound 14 was cocrystallized with CDK2, whereas 37 was soaked in existing CDK2 crystals. Prior to data collection, the crystals were transferred to a cryo-buffer containing PEG 3350 (10%) and glycerol (~25%) at pH 7.8 and were then flash-cooled in a cold nitrogen stream. Intensity data for 14 was collected at the synchrotron at the ESRF in Grenoble, and 37 was recorded on a rotating-anode system equipped with a three-circle diffractometer and Smart 6000 CCD area detector. The data for 14 were integrated with the HKL2000 package,^[27] data for 37 were integrated with the SAINT program and corrected semiempirically for systematic errors such as absorption with the program SADABS. Both structures were solved with the aid of the program AMoRe.^[28] Compound 14 was refined by use of SHELXL,^[29] whereas 37 was refined with the CNS module in the Quanta program.

The crystallographic data for both structures have been deposited with the Brookhaven Data Bank (PDB), Brookhaven National Laboratory, under the access codes 2BHE and 2BHH.

Selected Synthetic Procedures

Indirubin-5-sulfonyl chloride (21): Thionyl chloride (32 mL, 440 mmol, excess) was added slowly at RT to indirubin-5-sulfonic acid (20; 2 g, 5.48 mmol).^[7] The mixture was then stirred at 80°C for 3 h. After cooling down, it was cautiously poured into ice/water, and the mixture was stirred for an additional 20 min. The precipitate was filtered off, washed with water, and vacuum dried at RT to yield indirubin-5-sulfonyl chloride 21 (1.49 g, 4.13 mmol, 75%). ¹H NMR (400 MHz, [D₆]DMSO): δ = 7.04 (t, *J* = 7 Hz, 1H), 7.43 (d, *J* = 8 Hz, 1H), 7.60–7.55 (m, 2H), 7.66 (d, *J* = 7.5 Hz, 1H), 9.12 (d, *J* = 2 Hz, 1H), 11.03 (s, 1H), 11.05 ppm (s, 1H); ¹³C NMR (100 MHz, [D₆]DMSO): δ = 188.2, 171.0, 152.3, 141.6, 140.8, 138.3, 136.9, 126.8, 124.1, 122.5, 121.2, 120.4, 118.9, 113.3, 108.2, 106.3 ppm; MS (EI): *m/z* (%): 362 (40) [*M*]⁺, 360 (100) [*M*]⁺, 261 (40), 233 (35); HRMS (EI) C₁₆H₉N₂O₄SCI calcd: 359.9972; found 359.9965 [*M*]⁺.

Basic indirubin 22: A solution of indirubin-5-sulfonylchloride (21; 599 mg, 1.66 mmol), DMAP (30 mg, 0.25 mmol, 0.15 equiv), and *N,N,N*-trimethylethylenediamine (0.42 mL, 3.24 mmol, 2 equiv) in EtOH (10 mL) was stirred for 8 h at 60°C. After the mixture had cooled, the crystalline precipitate was filtered off, washed with water and with ethanol, and vacuum-dried at 60°C to yield 22 (601 mg, 1.47 mmol, 85%). ¹H NMR (300 MHz, [D₆]DMSO): δ = 2.77 (s, 3H), 2.83 (s, 6H), 3.3 (brs, 4H), 7.08 (t, *J* = 8 Hz, 1H), 7.13 (d, *J* =

8 Hz, 1H), 7.47 (d, *J* = 8 Hz, 1H), 7.62 (t, *J* = 8 Hz, 1H), 7.70–7.77 (m, 2H), 9.23 (d, *J* = 1 Hz, 1H), 11.23 (s, 1H), 11.47 ppm (s, 1H); ¹³C NMR (100 MHz, [D₆]DMSO): δ = 188.7, 170.7, 152.4, 143.6, 139.5, 137.2, 129.4, 128.0, 124.5, 123.1, 121.7, 121.6, 118.8, 113.5, 109.4, 104.2, 56.6, 47.4, 44.9, 35.0 ppm; MS (EI): *m/z* (%): 426 (7) [*M*]⁺, 425 (12), 384 (15), 383 (70), 276 (65), 275 (100); HRMS (EI) C₂₁H₂₂N₄O₄S calcd: 426.1362; found 426.1344 [*M*]⁺.

Quaternary indirubins 30a/30b: A solution of methylmagnesium bromide in diethyl ether (3 M, 1 mL, 3 mmol, 1 equiv) was added slowly to a cold (+4°C) solution of basic indirubin 22 (1.28 g, 3.0 mmol) in pyridine (50 mL) and THF (25 mL). Afterwards, the mixture was stirred for 30 min at RT. The mixture was then poured into a cold (0°C), saturated ammonium chloride solution, diluted with water, and extracted with AcOEt (3×). The combined organic layer was dried (MgSO₄) and concentrated. The residue was purified by flash chromatography (silica gel, CH₂Cl₂→CH₂Cl₂/MeOH 4:1) to afford the racemic mixture 30a/30b (595 mg, 43%). This material was subjected to preparative chiral HPLC (Chiralpak AS 10μ, hexane/EtOH 2:1) to yield 30a (209 mg, 15%, 0.45 mmol) and 30b (215 mg, 15%, 0.46 mmol).

Compound 30a: [α]_D²² = +286.8 (*c* = 0.15, MeOH); ¹H NMR (400 MHz, [D₆]DMSO): δ = 2.13 (s, 6H), 2.38 (t, *J* = 7 Hz, 2H), 2.84 (dd, *J* = 13 Hz, 8 Hz, 1H), 2.94–3.03 (m, 3H), 4.82 (d, *J* = 17.5 Hz, 1H), 4.92 (dd, *J* = 10.5 Hz, 2 Hz, 1H), 5.36–5.46 (m, 1H), 6.80 (s, 1H), 7.00–7.04 (m, 2H), 7.22–7.30 (m, 2H), 7.40–7.43 (m, 2H), 8.63 (d, *J* = 2 Hz, 1H), 10.94 (s, 1H), 11.33 ppm (s, 1H); ¹³C NMR (100 MHz, [D₆]DMSO): δ = 169.9, 164.3, 142.4, 140.2, 133.0, 131.0, 129.1, 127.7, 123.3, 123.1, 123.0, 122.0, 121.0, 119.2, 111.4, 108.4, 94.6, 82.1, 56.6, 47.5, 44.9, 40.8, 35.0 ppm; MS (EI): *m/z* (%): 468 (6) [*M*]⁺, 427 (85), 425 (50), 383 (15), 254 (100); HRMS (EI) C₂₄H₂₈N₄O₄S calcd: 468.1831; found 468.1834 [*M*]⁺.

Compound 30b: [α]_D²² = –286.4 (*c* = 0.17, MeOH); all other analytical data identical to 30a.

Acknowledgements

We would like to thank M. Möwes and K. Joachim for technical support, U. Ganzer for physicochemical characterization of the compounds, and U. Ebespächter for protein production of CDK2.

Keywords: biological activity · enzymes · medicinal chemistry · natural products · structure–activity relationships

- [1] J. Balfour-Paul, *Indigo*, British Museum Press, London, 1998.
- [2] A. von Bayer, P. Emmerling, *Ber. Dtsch. Chem. Ges.* **1870**, 515.
- [3] L. M. Wu, Y. P. Yang, Z. H. Zhu, *Comm. Chin. Herb. Med.* **1979**, 9, 6.
- [4] K.-M. Wu, M.-Y. Zhang, Z. Fang, L. Hunag, *Yaoxue Xuebao* **1985**, 20, 821.
- [5] Y. C. Gu, G. L. Li, Y. P. Yang, J. P. Fu, C. Z. Li, *Yaoyue Xuebao* **1989**, 24, 629.
- [6] R. Han, *Stem Cells* **1994**, 12, 53.
- [7] R. Hoessel, S. Leclerc, J. A. Endicott, M. E. M. Nobel, A. Lawrie, P. Tunnah, M. Leost, E. Damiens, D. Marie, D. Marko, E. Niederberger, W. Tang, G. Eisenbrand, L. Meijer, *Nat. Cell Biol.* **1999**, 1, 60.
- [8] A. Huwe, R. Mazitschek, A. Giannis, *Angew. Chem.* **2003**, 115, 2170; *Angew. Chem. Int. Ed.* **2003**, 42, 2122.
- [9] W. Grell, R. Walter, A. Heckel, F. Himmelsbach, H. Wittneben, J. v. Meel, N. Redemann, R. Haigh, in *PCT WO9951590*, 1999.
- [10] S. C. Conway, G. W. Gribble, *Heterocycles* **1990**, 30, 627.
- [11] T. G. Davies, P. Tunnah, L. Meijer, D. Marko, G. Eisenbrand, J. A. Endicott, M. E. M. Noble, *Structure* **2001**, 9, 389.
- [12] S. H. Yalkowski, S. C. Valvani, *J. Pharm. Sci.* **1980**, 69, 912.
- [13] H. van de Waterbeemd, D. A. Smith, K. Beaumont, D. K. Walker, *J. Med. Chem.* **2001**, 44, 1313.

- [14] M. Y. Tesconi, H. Samuel in *Handbook of Property Estimation Methods for Chemicals* (Ed.: R. S. M. Boethling, D. C. Donald), Lewis, Boca Raton, FA, **2000**, p. 3.
- [15] S. J. Danishefsky, M. J. O. Grandi, C. A. Coburn, R. C. A. Isaacs, *J. Org. Chem.* **1993**, *58*, 7728.
- [16] S. Leclerc, M. Garnier, R. Hoessel, D. Marko, J. A. Bibb, G. L. Snyder, P. Greengard, J. Biernat, Y.-Z. Wu, E.-M. Mandelkow, G. Eisenbrand, L. Meijer, *J. Biol. Chem.* **2001**, *276*, 251.
- [17] L. Meijer, A.-L. Skaltsounis, P. Magiatis, P. Polychronopoulos, M. Knockaert, M. Leost, X. P. Ryan, C. A. Vonica, A. Brivanlou, R. Dajani, *Chem. Biol.* **2003**, *10*, 1255.
- [18] J. Adachi, Y. Mori, S. Matsui, H. Takigami, J. Fujino, H. Kitagawa, C. A. Miller III, T. Kato, K. Saeki, T. Matsuda, *J. Biol. Chem.* **2001**, *276*, 31 475.
- [19] F. P. Guengerich, M. V. Martin, W. A. McCormick, L. P. Nguyen, E. Glover, C. A. Bradfield, *Arch. Biochem. Biophys.* **2004**, *423*, 309.
- [20] K. Sugihara, S. Kitamura, T. Yamada, T. Okayama, S. Ohta, K. Yamashita, M. Yasuda, Y. Fujii-Kuriyama, K. Saeki, S. Matsui, T. Matsuda, *Biochem. Biophys. Res. Commun.* **2004**, *318*, 571.
- [21] M. Knockaert, M. Blondel, S. Bach, M. Leost, C. Elbi, G. L. Hager, S. R. Nagy, D. Han, M. Denison, M. Ffrench, X. P. Ryan, P. Magiatis, P. Polychronopoulos, P. Greengard, L. Skaltsounis, L. Meijer, *Oncogene* **2004**, *23*, 4400.
- [22] T. D. Bradshaw, V. Trapani, D. A. Vasselin, A. D. Westwell, *Current Pharmaceutical Design* **2002**, *8*, 2475.
- [23] S. Safe, A. McDougal, *Int. J. Oncol.* **2002**, *20*, 1123.
- [24] S. L. McGovern, B. K. Shoichet, *J. Med. Chem.* **2003**, *46*, 1478
- [25] J. Seidler, S. L. McGovern, T. N. Doman, B. K. Shoichet, *J. Med. Chem.* **2003**, *46*, 4477.
- [26] For a recent related work on indirubins that acknowledges the importance of solubility but does not address this aspect, see: P. Polychronopoulos, P. Magiatis, A.-L. Skaltsounis, V. Myrianthopoulos, E. Mikros, A. Tarricone, A. Musacchio, S. M. Roe, L. Pearl, M. Leost, P. Greengard, L. Meijer, *J. Med. Chem.* **2004**, *47*, 935.
- [27] Z. Otwinowski, W. Minor, *Methods Enzymol.* **1997**, *276*, 307.
- [28] J. Navaza, *Acta Crystallogr. A* **1994**, *50*, 157.
- [29] G. M. Sheldrick, T. R. Schneider, *Methods Enzymol.* **1997**, *277*, 319.

Received: April 19, 2004